12 Mar 1991, 2:30 pm - 3:30 pm

Shaft Resistance During Driving in Clay from Laboratory Tests

A. Ben Amar
Laboratoire Central des Ponts et Chaussées, Nantes, France

D. Levacher
Ecole Nationale Supérieure de Mécanique, Nantes, France

Ph. Lepert
Central des Ponts et Chaussées, Nantes, France

P. Boisard
Société Nationale Elf Aquitaine, Pau, France

Proceedings: Second International Conference on Recent Advances in Geotechnical Earthquake Engineering and Soil Dynamics, March 11-15, 1991, St. Louis, Missouri, Paper No. 2.27

Shaft Resistance During Driving in Clay from Laboratory Tests

A. Ben Amar
Thesis Student, Laboratoire Central des Ponts et Chaussées, Nantes, France

D. Levacher
Formerly Lecturer, Ecole Nationale Supérieure de Mécanique, Nantes, France

Ph. Lepert
Engineer, Laboratoire Central des Ponts et Chaussées, Nantes, France

P. Boisard
Engineer, Société Nationale Elf Aquitaine, Pau, France

SUMMARY : This paper presents a laboratory study which aimed at investigating the soil/pile interaction during driving. A short review of past experimental works justifies the need for more consistent data. The test equipment (a rod driven through a sample of soil) is briefly presented and some signals are displayed to illustrate the quality of the measurements. The tests were performed on samples of normally consolidated Kaolinit clay. The analysis of the stress waves propagating in the rod, during driving, provided a good estimation of interaction forces, bar velocities and displacements of the pile model in the sample. Relationships were established between the interaction force, the energy dissipated in the sample of soil, the velocity and the displacement of the rod, and the confining pressure of the sample. Observations and relationships were used (1) to identify the physical phenomena occuring at the soil/pile interface during driving, and (2) to base a law governing this shaft interaction.

I - INTRODUCTION

The bearing capacity of pile can be roughly estimated from dynamic measurements using the stress wave theory. But this approach requires to know the laws governing the pile/soil interaction during driving.

The first, Smith (1960) proposed a visco-elastic model to describe this interaction, as a part of its famous although empirical framework to simulate pile driving on a computer. Most of later works aimed at improving the estimate of the parameters of this model. Only a few experimental studies have been actually devoted to carry out more realistic models based on a better understanding of the physical phenomena occuring at the soil / pile interface. Mizikos and Fournier (1980), Jaï (1983), Meynard and Corté (1984), and Middendorp and Van Brederode (1984) presented such an approach, focusing their efforts on shaft interactions. They founded their works on laboratory tests, using scale models which were basically similar : small hammers or falling rams were used to drive a long steel rod through a sample of soil located at its midlength. The normal stresses were measured in two or three sections of the rod, outside of the sample, using strain gages. In most cases, the transient displacement of another section (outside of the sample too) was recorded too. Surprisingly quite different, when not contradictory, interaction models were derived from these similar experiments. For sand / pile shaft interaction, Jaï (1983) proposed a purely rigid-plastic law, while Meynard and Corté (1984) recognized a linear relationship between the interaction force and the pile velocity. On their side, Middendorp and Van Brederode (1984) derived from their study a more complicated model combining springs, dashpots and masses. In fact, a carefull examination of the published papers (Lepert et al., 1988 a) showed that these conclusions were largely depending on the experimental conditions and on the procedures of interpretation. This examination enlightened some factors which had drastic impacts on the reliability and consistancy of the conclusions :

- length of the rod,
- size and location of the sample, with respect to the rod,
- control of soil parameters (stress distribution in the sample, density, ...)
- shape and characteristics of the incident stress wave,
- sensitivity of the sensors,
- interpretation of the strain gages signals,
- etc.

In 1986, a new test equipment was designed and realized, on the basis of concepts wich took into account the past experiences, especially with respect to the former points. It was extensively described in a previous paper, by Lepert et al. (1988.a). The first experiments were conducted on dry sandy samples, and led to encouraging results (see Lepert et al, 1988.b). In a second step of the study, experiments were performed on normally consolidated clay samples, in drained conditions.

After a short presentation of the test equipment, this paper displays some results from the tests on clay samples, and derives a law for clay / pile shaft interaction. Emphasis is put on the fact that this law must be completed by a model which describes the radiation of energy in the soil.

II - THE EXPERIMENTAL SET-UP

The pile model is a 9 m long steel rod, 0.02 m in diameter, installed in a vertical position. The upper half is hung above the ground level to a scaffolding, while the lower half is in a cased drill-hole (see fig. 1). Thus, apart from two very flexible elastics, which links the scaffolding to the rod, the later is completly free outside the soil sample.

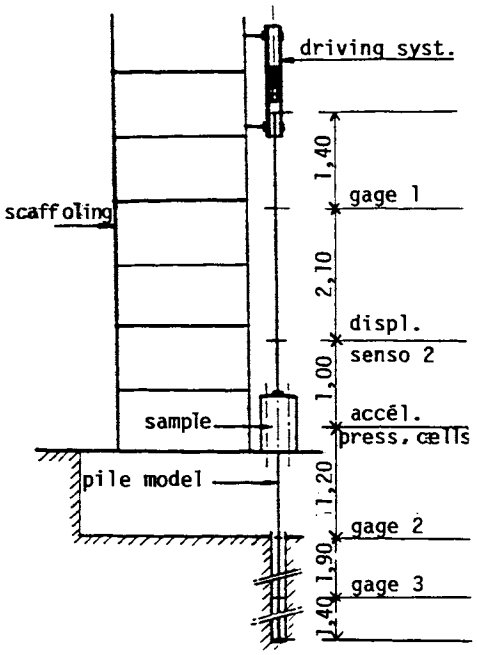

Figure n° 1 : the test equipment with the location of the different sensors

The "driving system" is composed of a 3 m long tube, partly surrounding the top of the rod, and guiding a free falling mass which impacts the rod. Various falling masses are available, which are made with the same material and have the same cross section than the rod. The impact of such masses onto the rod produces a rectangular shock. Its duration is proportionnal to the length of the mass (ranging from 0.3 to 1.65 m) and its amplitude is proportionnal to the height of the fall (up to 2.0 m).

The soil sample must be long enough to applied a significant lateral resistance on the rod, even when the confining pressure is low. On the other hand, a long sample would create long resistance waves which might inextricabily overlap in the rod. It would also no longer support the assumption of concentrated soil / pile interaction. So, a height of 0.50 m appears as a good compromise between these opposite requierements. The diameter of the sample is 0.2 m, and it is jacketed in a thin rubber membrane coated inside with a geotextile. It is capped top and down by circular porous platterns.

The clay samples are made of kaolinite (see next §) prepared at 90% water content. This homogeneous material is uniformly poured in a special mold, directly at its final place around the rod (fig. 2a). An annular hydraulic jack acting on a piston is vertically loading the sample and thus consolidating it to the desired degree, under oedometric conditions. At the end of this phase, the mold is removed and replaced by a triaxial cell surrounding the sample (fig. 2b). The tests are thus performed under triaxial conditions.

The different sensors implemented on the test equipment are located on Fig. 1. Strain gages are glued onto the rod in three sections, one above the soil sample and the two others below it. The location of the upper and lower sections is such that the stress waves travelling in the rod does not overlap at any time in these sections. The transient displacement of a fourth section is measured using an opto-electronic sensor. All sensors have a very high resolution (a few Newtons for the strain gages, a few microns for the displacement sensor) and their frequency bandwith is 0 - 20 kHz. They are connected, through appropriate amplifiers, to a multi-channels transient data recorder. The analog signals are digitized in parallel with a 10 bits ADC system and stored in a 8 K-words memory. The sampling frequency is 200 kHz. Once the data acquisition is completed, the mesurements are transfered to a micro-computer and stored on floppy disks.

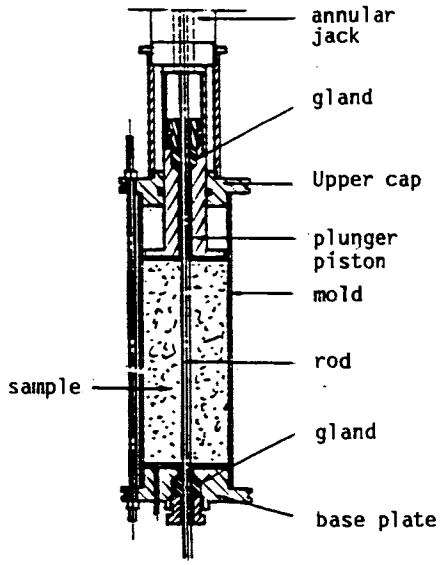

Figure n° 2a : the oedometric mold used to prepare clay samples

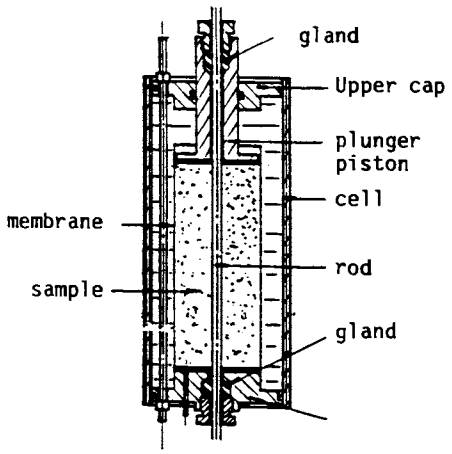

Figure n° 2b : the triaxial cell surrounding the sample during the test

III - TESTED MATERIAL

The tested material is reconstituted in laboratory from natural clay powder. This 100% kaolinit clay is coming from Brittany (see table I).

TABLE I. Kaolin references

mix	origin (%)	reference
100	Ploërmel natural kaolin	Kaolin KP

Kaolin and water are vacuum mixed with a mixing machine at constant speed. The initial water content is about 90%, i.e , 22 liters of water for 25 kg of kaolin. The mix duration is 2 hours long. The reconstituted clay is poured in the oedometric mould (see fig. 2a) and is consolidated under a 300 kPa pressure. This consolidation can be completed in isotropic conditions in the range 300-500 kPa, according to the tests to be carried out.

Various laboratory tests have been performed to characterize this material in test conditions. Table II presents its physical and mechanical properties.

TABLE II. Reconstituted clay characteristics

Physical properties	Plasticity limit (%)	$W_p = 31$
	Plasticity index	$I_p = 23$
Mechanical properties	Compression index	$C_c = 0.70$
	Expansion index	$C'_c = 0.13$
	Shear strength[1](kPa) C_u = 64-67 [water content (%) W^u = 38.5-40]	
	Shear strength[2](kPa) C_u = 65.5 [water content (%) W^u = 38.5-40]	

[1] from scissometer tests on reconstituted clay, normally consolidated at 300 kpa.

[2] from U.U. triaxial tests.

Since the consolidation is directly made around the rod, it is impossible to perform any test of soil mechanics on the sample just after consolidation. But, at the end of each experiment, the homogeneity of the reconstituted clay sample is checked, and then the water content and undrained shear strength are measured. The results are recapitulated in table III.The scattering of water content is small, indicating that the procedure of preparation of the sample is reproductive and that the samples themselves are homogeneous. Furthermore, the shear strength of the clay calculated with formula :

$$C_u = 0.2\ \sigma'_v\ (OCR)^{0.6} \qquad (1)$$

is close to the values given in table II.

TABLE III. Water content measurements

Sample number	Confining pressure kPa	Water content W (%)	Shear strength C_u (kPa)
1	500	32.9-34.5	-
2	500	34.5-35.3	73.1
3	500	32.7-34.4	-

IV - PRESENTATION AND PROCESSING OF SIGNALS

Fig. 3 is a diagram of the propagation of stress waves in the rod after the impact of a falling mass. It enables a quick and easy qualitative interpretation of the signals from the different sensors.

IV.1 Presentation of gages signals

Fig. 4 shows typical normal stress signal measured in a section of the rod above the sample. The first incident wave coming from the top of the rod (peak A) mobilizes a resistant force between the soil and this rod when it crosses the sample. This force generates in turn a resistant wave travelling upward (peak B). Both waves are reflected at the rod extremities and cross again the sample where they exchange some energy. At each time, the amplitude of the incident wave decreases while the resistant wave increases by the same amount. After a number of passages through the sample, the incident and resistant waves are balanced and decrease together untill being completely damped out.

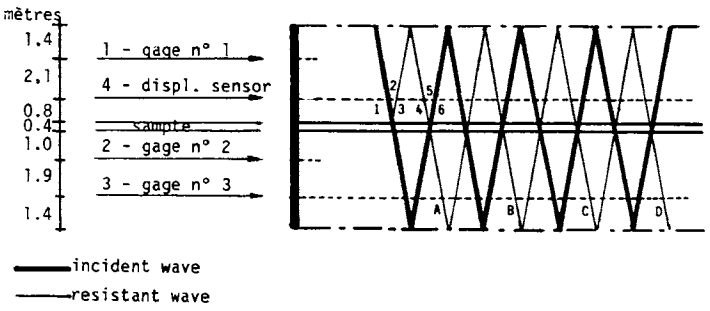

Figure n° 3 : diagram of the propagation of waves in the rod

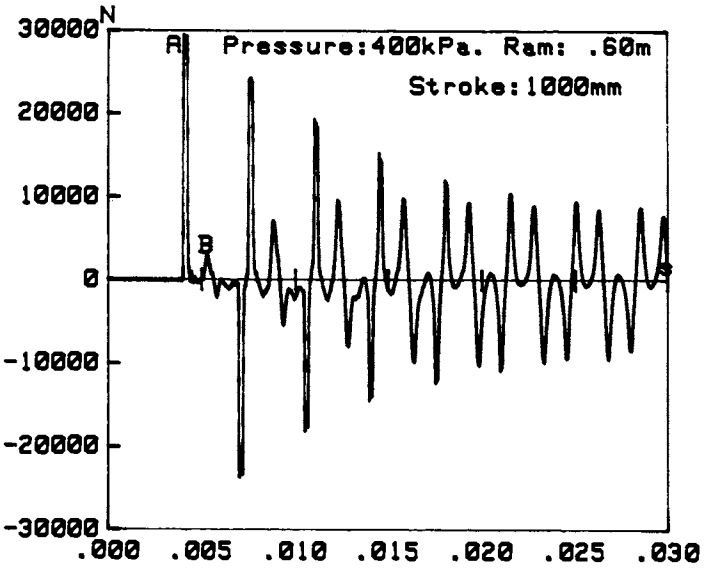

Figure n° 4 : typical normal stress signal.

IV.2 Computation of interaction force

A first method was developped to derive the amplitude of the soil/pile interaction force from the gages signals. It took fully into account both the duration of the waves and the exact length of the sample. The latter was divided into a number of sublayers in which the stresses equilibrium and velocity continuity relationships were applied. Using this detailed but rather complicated method, it could be proved that, in the usual range of experimental conditions, the interaction force could be regarded

as a concentrated one, located in the middle section of the sample. This observation led to significant simplifications of the interpretation method. Let us call (see fig. 3) :

Fo = incoming incident wave,
F1 = outgoing incident wave,
Go = incoming resistant wave, } (>0 in compression)
G1 = outgoing resistant wave,
R = soil / pile interaction force. (>0)

It can be demonstrated that, under the assumption of a concentrated interaction and provided Fo - Go > R/2, the following relationships holds true :

$$F1 - Fo = - R / 2 \qquad (2a)$$
$$G1 - Go = R / 2 \qquad (2b)$$

Hence, the shaft resistance R amplitude can be directly derived from the peak values of the measured incident and resistant waves. For conveniency, the following relation was used :

$$R = (F_0 - F_1) + (G_1 - G_0) \qquad (3)$$

IV.3 Computation of the bar velocity in the sample

Since the different stress waves don't overlap in the measurement sections, the bar velocity in these sections V can easily be derived from the normal force F through the relationship :

$$V = \varepsilon F / Z \qquad (4)$$

where :

ε = -1 for upward travelling waves
ε = 1 for downward travelling waves
Z = mechanical impedance of the rod

On the contrary, the waves are always overlapping in the sample (they are crossing one another). Therefore, we compute the bar velocity in this sample as the average of the bar velocities in the measurement sections, above and below the soil sample, before and after the passage of the wave through the sample :

$$V = (F_0 - G_1 + F_1 - G_0) / 2 Z \qquad (5)$$

IV.4 Transient displacement signal

A typical transient displacement signal measured above the sample is presented in fig. 5. One should notice that, in this case, the different waves partially overlap in the measured section. The first downward step (1-2) is caused by the passage in the section of the first compressive incident wave. The following upward step (2-3) results from the upward passage of the first compressive resistant wave.

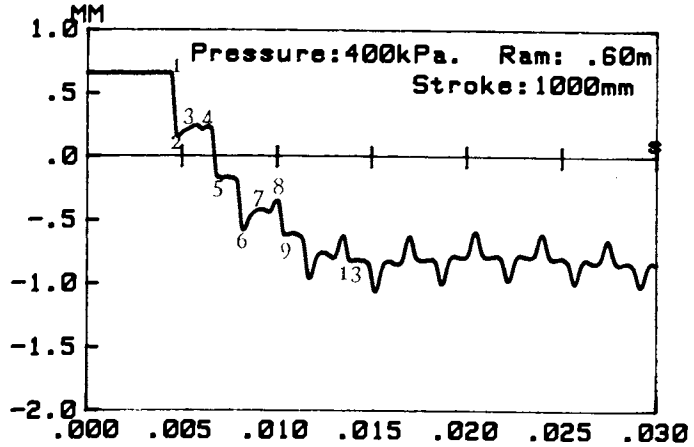

Figure n° 5 : typical displacement signal.

After reflection at the top extremity of the rod, the resistant wave, now a tensile wave, crosses again the measurement section and causes the upward step displacement (3-4). Finally, the incident wave, a tensile stress wave after reflection at the bottom extremity of the rod, propagates upward and creates the downward step displacement (4-5). Then the whole step (1-5) corresponds to the displacement of the rod after a complete return travel of the waves . The same analysis applies for the second passage of the waves (5-9), for the third one (9-13), and so on...These steps are called the "unit displacements" in the subsequent sections.

The unit displacement can also be calculated as the sum of the integrals, over the wave duration, of the terms of eq. 5 . The comparison of the results given by the two methods (fig. 6) shows a good agreement between the values.

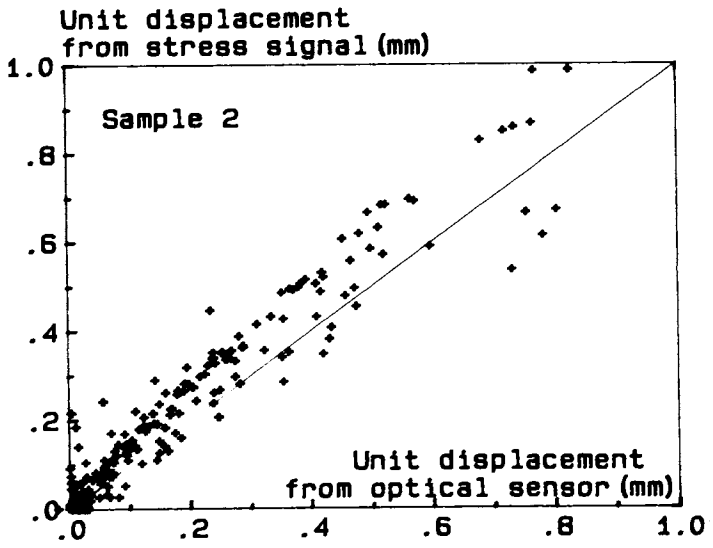

Figure n° 6 : unit displacements measured with the opto-electronic sensor versus unit displacement derived from normal stress signals.

IV.5 Estimate of energy

The energy E(F) associated with a stress wave F can be derived from the stress signal through the integral :

$$E = \int_0^t \sigma^2 / Z \, dt \qquad (6)$$

where

t is the wave duration
σ is the stress wave amplitude

The energy which dissipated in the sample during a return travel of the waves is the difference between the energy conveyed by waves coming in the sample and the energy taken away by the outgoing waves:

$$\Delta E = E(F_0) + E(G_0) - E(F_1) - E(G_1) \qquad (7)$$

V - INTERPRETATION OF RESULTS

V.1 Effect of the bar velocity on the shaft resistance

It was commonly reported in the past studies (Litkouhi and Poskitt, 1980, Dayal and Allen, 1975, Heerema, 1979) that the bar velocity was a predominant factor in the mobilisation of the shaft resistance. Figure n° 7 presents the variation of this shaft resistance with the bar velocity, for several shocks given by a mass falling from various heights. The points with the same symbol correspond to the successive passages of the waves

through the sample after a shock while different symbols hold for shocks from various heights. According to this diagram, the shaft resistance seems to increase asymptotically with the bar velocity. The following function correctly fit the experimental points :

$$R = A\,(1 - \exp(-BV)) \qquad (8)$$

In principle, A and B are coefficients depending on the duration of impact, the confining pressure and the properties of the soil. A large number of tests were performed on several kaolinite samples in which the length of the falling mass (i.e. the duration of the impact) and the confining pressure were varied. A et B were computed in each case using a non linear regression method. A range of uncertainty was associated with each value by processing the standard deviation of the non-linear regression. Fig. 8 displays the variations of the parameters A and B with the length of the falling mass (i.e. the duration of the impact) and the confining pressure.

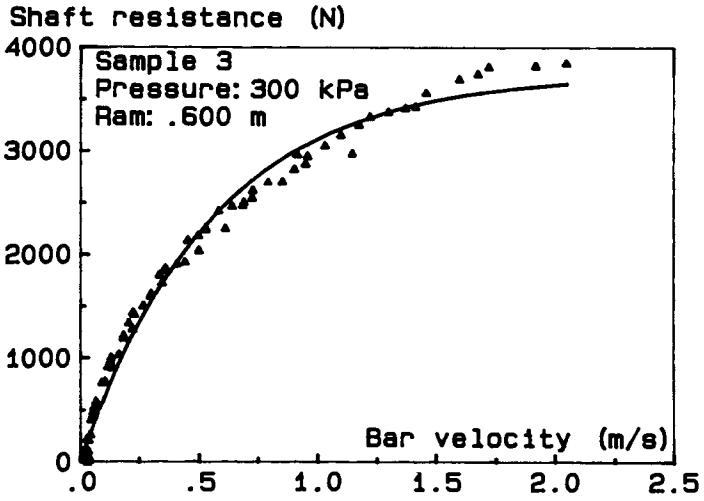

Figure n° 7 : shaft resistance versus bar velocity

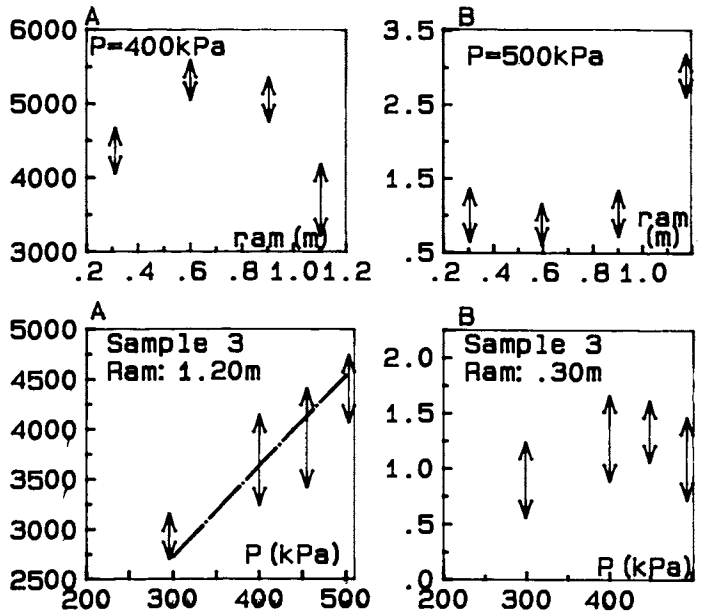

Figure n° 8 : variations of the coefficients A and B with the length of the ram and the confining pressure of the sample

According to these figures, it may be stated that A increases linearly with the confining pressure P. But no clear relationships can be stated between :

A and the length of the falling mass on one side,
B and the length of the falling mass or the confining pressure on the other side,

even if the incertainties on the values are taken into account.

V.2 Dissipated energy versus bar velocity relationship

At each time the stress waves pass through the sample, a certain amount of energy is dissipated either in friction between the rod and the sample or by internal damping in the soil. This energy, ΔE, caculated using eq. (7), may be drawn as a function of the bar velocity V. A typical example of this function is shown on figure 9, which displays results from the tests.

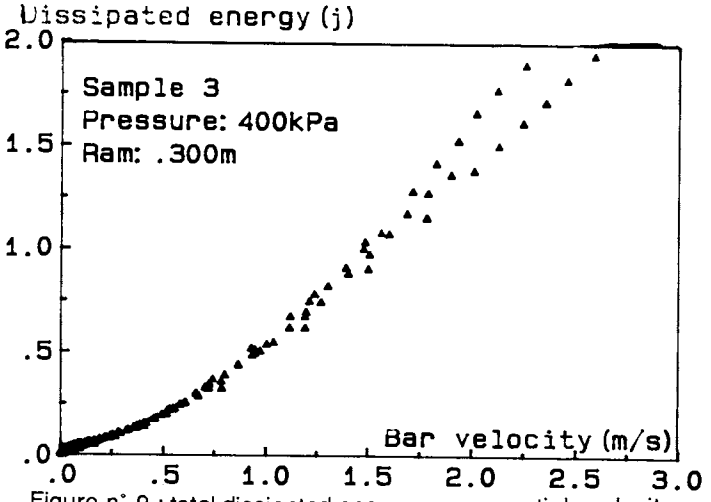

Figure n° 9 : total dissipated energy versus particle velocity.

The best fit of this relationships was obtained with a power function :

$$\Delta E = \mu V^{\alpha} \qquad (9)$$

The exponent α remains constant and equal to 1.5 for all the tests performed on normally consolidated clays. The μ coefficient was found to linearly depend on the hammer length L and on the confining pressure P. In other terms, it can be expressed as :

$$\mu = \lambda P L \qquad (10)$$

where λ is a dimensional parameter depending only on the material of the sample. This relationship is confirmed by figure 10, which displays the variation of $\lambda = \Delta E / PLV^{\alpha}$ as a function of V for all the tests, whatever are the confining pressure, the length of the ram and the height of fall.

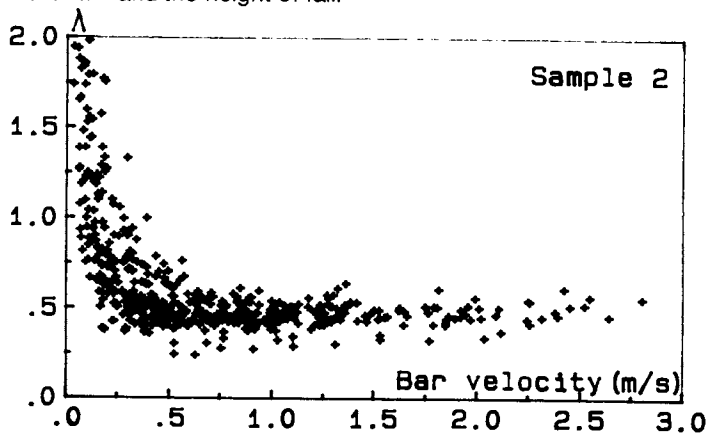

Figure n° 10 : λ versus bar velocity curve

It clearly shows that, for all the tests performed on normally consolidated clays, λ is constant at least beyond a critical particle velocity V_c. The scattering of the points under this value is probably due to some lack of accuracy of the interpretation in the small velocities range.

V.3 Unit displacement versus bar velocity relations

The unit displacement is defined and calculated as explained in § IV.4. The relation between this unit displacement and the bar velocity is drawn on figure 11 from tests on sample n° 3 driven under a confining pressure of 500 kPa, with rams of different lengths falling from various heights.

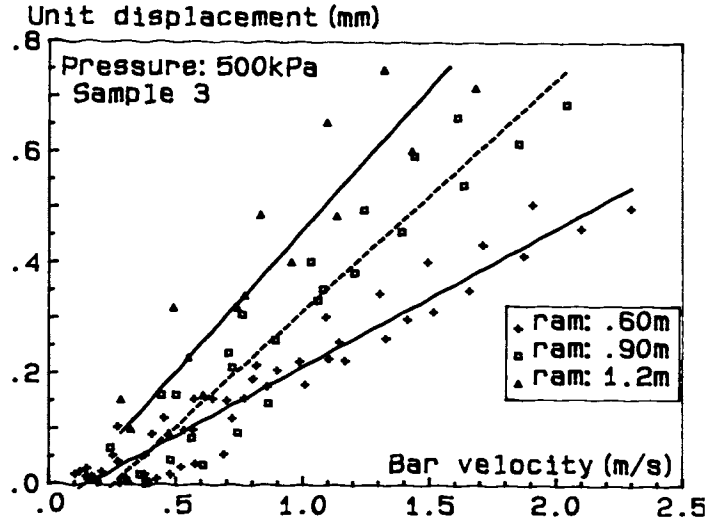

Figure n° 11 : unit displacement versus bar velocity

According to figure 11, the unit displacement D is a linear function of the bar velocity V. The slope D/V is proportionnal to the length of the hammer as shown on figure 11. A closer examination of this slope shows that the following relationship holds true :

$$D = T_i \cdot V \qquad (11)$$

where T_i is the duration of the impact generated by the hammer n° i onto the rod.

VI - SHAFT INTERACTION LAW

It is a practical evidence that a soil / pile interaction law is useable for numerical simulation of driving only if it involves a limited number of well chosen parameters. Furthermore, these parameters must characterize the state of the soil (material, density, stress or strain fields,...) and the state of the pile in the section under consideration (velocity, displacement, stress,...). Parameters which depends on the interface history are more difficult to handle. In any case, global quantities such as the whole duration of the impact are not adequat parameters for a law to be used within the context of incremental computations.

VI.1 Derivation of a law

As seen in § V.1, there is no physical evidence of the influence of the duration of the pile/soil interaction on the amplitude of this interaction. Therefore, in order to propose a simple and useable shaft interaction law, the following relationships were derived from § V.1 :

$$A = a\,P \qquad (12\,a)$$
$$B = b = \text{const.} \qquad (12\,b)$$

where a and b are two constants depending only on the soil material and density. As a consequence, the instantaneous shaft resistance is only depending on the soil material and on the bar velocity through the relationship :

$$R = aP\,(1 - \exp(-bv)) \qquad (13)$$

VI.2 Validation of the law

In order to validate this relationship, it was rearranged as:

$$R / P = a(1-\exp(-bv)) \qquad (14)$$

and applied for all the measures carried out on each clay sample disregarding the falling mass length, the confining pressure, the height of the fall. The result presented in fig. 12 shows that there is enough consistency to consider that the relation above represents faithfully the influence of bar velocity on the shaft resistance in any tested conditions.

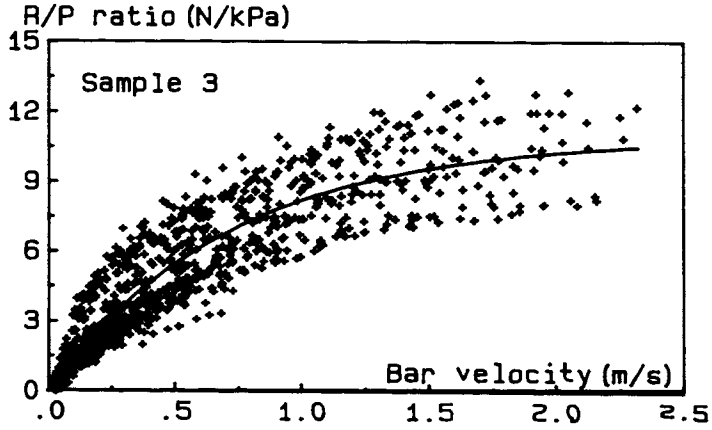

Figure n° 12 : R / P ratio as a function of the bar velocity for all the tests on clay sample n° 1

Figure n° 13 compares the energy dissipated by friction between the rod and the sample at each passage of the waves (estimated as $E_f = D \cdot R$) and the total energy dissipated during this passage (see § IV.5). This diagram still shows a good consistency in the results as the energy dissipated by friction is about 80% of the total energy in the interaction.

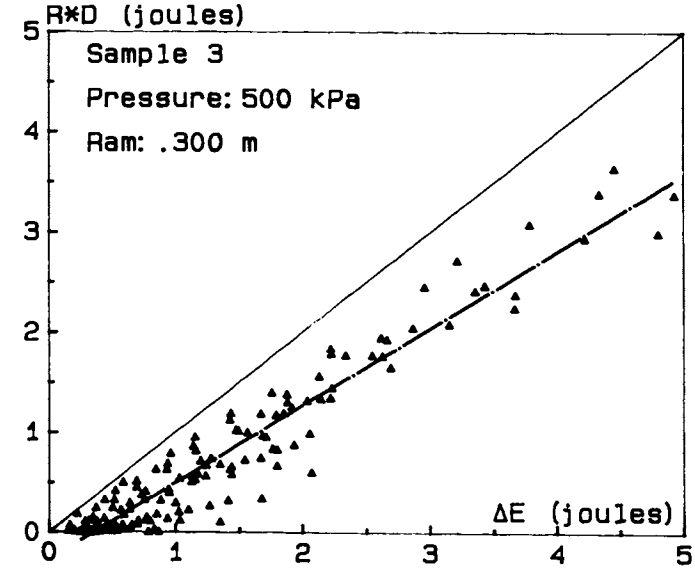

Figure n° 13 : Energy dissipated by friction between the rod and the sample versus total energy dissipated in the interaction process

VII - CONCLUSIONS

As emphasized by Corté et Lepert (1986), the soil / pile interaction model should involved two stages :

- the first one describes the behaviour of the interface itself, including a thin layer of soil in the vicinity of the pile where almost pure shear is developped,

- the second one modelizes the radiation of energy by elastic shear waves travelling in radial direction, in an outer zone.

The results from this experimental study suggest that the first stage of this interaction model might essentially be of friction type. But they also show that the amplitude of this friction is a function of the differential velocity between the pile section and the surrounding soil. Equation (13) provides a good representation of this function, with only two parameters depending on the soil properties. The second stage of the model remains a visco-elastic model as proposed by Corté et Lepert (1986).

REFERENCES

CORTE J.F. , LEPERT P.,1986. Lateral resistance during driving and dynamic pile testing, Proc. 3rd International conference on numerical methods in offshore piling, Nantes (France), pp 19-33.

DAYAL U. , ALLEN J.H., 1975. The effect of penetration rate on the strength of remolded clay and sand samples, Canadian Geotechnical Journal, Vol. 12 , N° 3 , pp 336-348

HEEREMA E.P., 1979. Relationships between wall friction, displacement, velocity, and horizontal stress in clay and in sand, for pile driveability analysis, Ground Engineering, Jan., pp 55-65

JAI A., 1983. Contribution à l'étude de la capacité portante des fondations profondes pendant le battage, Thesis, Ecole Centrale des Arts et Manufactures de Paris.

LEPERT P., CORTE J-F., GOULOIS A., MEUNIER J., 1988.a Shaft resistance during driving, for sand, from laboratory tests, Proc. 3rd International Conference on the Application of Stress-Wave-Theory on Piles, Ottawa, May, pp 431-440.

LEPERT P., CORTE J-F., GOULOIS A., 1988.b An experimental set-up for investigation of shaft resistance during driving, Proc. 3rd International Conference on the Applicatiion of Stress-Wave-Theory on Piles, Ottawa, May pp 422-430.

LITKOUHI S. , POSKITT T.J., 1980. Damping constants for pile driveability calculations, Geotechnique, Vol 30, N° 1, pp 77-86.

MEYNARD A., CORTE J-F., 1984. Contribution à l'étude des lois d'interaction sol / pieu pour l'analyse des essais de battage de pieu, Rapport de recherche LPC N° 133, Octobre, Paris.

MIDDENDORP P., VAN BREDERODE P.J., 1984. Skin Friction Models for Sand from Static and Dynamic Laboratory Tests, 2nd International Conference on the Application of Stress-Wave-Theory on Piles, Stockholm.

MIZIKOS J.P., FOURNIER J., 1980. From driving to pile foundations : a first step for clays, Proc. 1st International Conference on the Application of Stress-Wave-Theory on Piles, Stockholm, pp 233-256.

SMITH E.A.L., 1960. Pile driving analysis by the wave equation, Journal of the Soil Mechanics and Foundations Division, Proc. ASCE, Vol. 86, SM4, pp 35-61.